JCB Article

ARF6 controls post-endocytic recycling through its downstream exocyst complex effector

Magali Prigent,[1] Thierry Dubois,[1] Graça Raposo,[2] Valérie Derrien,[1] Danièle Tenza,[2] Carine Rossé,[3] Jacques Camonis,[3] and Philippe Chavrier[1]

[1]Membrane and Cytoskeleton Dynamics Group, [2]Electron Microscopy Laboratory, Centre National de la Recherche Scientifique, UMR-144, and [3]Institut National de la Santé et de la Recherche Médicale, U-528, Institut Curie, F-75248 Paris Cedex 05, France

The small guanosine triphosphate (GTP)–binding protein ADP-ribosylation factor (ARF) 6 regulates membrane recycling to regions of plasma membrane remodeling via the endocytic pathway. Here, we show that GTP–bound ARF6 interacts with Sec10, a subunit of the exocyst complex involved in docking of vesicles with the plasma membrane. We found that Sec10 localization in the perinuclear region is not restricted to the *trans*-Golgi network, but extends to recycling endosomes. In addition, we report that depletion of Sec5 exocyst subunit or dominant inhibition of Sec10 affects the function and the morphology of the recycling pathway. Sec10 is found to redistribute to ruffling areas of the plasma membrane in cells expressing GTP-ARF6, whereas dominant inhibition of Sec10 interferes with ARF6-induced cell spreading. Our paper suggests that ARF6 specifies delivery and insertion of recycling membranes to regions of dynamic reorganization of the plasma membrane through interaction with the vesicle-tethering exocyst complex.

Introduction

To form membrane extensions such as lamellipodia at the leading edge of migrating cells, local polymerization of actin filaments must be coordinated with polarized insertion of membrane components. It has long been proposed that membranes inserted at the leading edge would be derived from the recycling of surface components, internalized via the endocytic pathway (Bretscher, 1996). Transferrin receptors (TfRs), which are internalized via clathrin-coated pits and delivered to tubulo-vesicular recycling endosomes (REs), have been shown to recycle back from REs and accumulate at the leading edge of migrating fibroblasts (Hopkins et al., 1994). More recently, polarized recycling to the leading edge has been reported for integrin receptors, and for the v-SNARE protein VAMP3, a marker for REs (Daro et al., 1996), during phagocytosis in macrophages (Bajno et al., 2000; Pierini et al., 2000; Laukaitis et al., 2001; Roberts et al., 2001; Niedergang et al., 2003). All together these observations indicate that the RE may serve as a storage compartment regulating the availability of plasma membrane lipid and protein components needed for cells undergoing changes in morphology (Lecuit and Pilot, 2003). However, little is yet known about how post-endocytic recycling is polarized in order to contribute to local membrane delivery at specialized plasma membrane locations.

ADP-ribosylation factor (ARF) 6, a member of the family of ARF small GTP-binding proteins, regulates membrane movement between the plasma membrane and early endocytic compartments (Chavrier and Goud, 1999). Like all small GTP-binding proteins, ARF6 cycles between active GTP and inactive GDP-bound forms, and studies from several laboratories have indicated that ARF6 activation occurs at the plasma membrane (D'Souza-Schorey et al., 1998; Frank et al., 1998; Franco et al., 1999; Vitale et al., 2002). The ARF6 GDP/GTP cycle has been shown to regulate the uptake and recycling of plasma membrane proteins to generate membrane protrusive structures concomitant with alterations in the cortical actin cytoskeleton (Radhakrishna and Donaldson, 1997; D'Souza-Schorey et al., 1998; Franco et al., 1999; Palacios et al., 2001). This specific and essential role of ARF6 is further reflected by its involvement in various cellular processes requiring transient cellular polarization such as cell spreading, cell motility and phagocytosis (Song et al., 1998; Zhang et al., 1998; Radhakrishna et al., 1999;

The online version of this article contains supplemental material.

Address correspondence to Philippe Chavrier, UMR144 Centre National de la Recherche Scientifique, Institut Curie, 26 rue d'Ulm, F-75248 Paris cedex 05, France. Tel.: 33-1-42-34-63-59. Fax: 33-1-42-34-63-77. email: philippe.chavrier@curie.fr

Key words: ARF6; exocyst complex; recycling; endocytosis; small GTP-binding protein

Abbreviations used in this paper: ARF, ADP-ribosylation factor; NRK, normal rat kidney; RE, recycling endosome; siRNA, small interfering RNA; Tf, transferrin; TfR, transferrin-receptor.

Palacios et al., 2001; Santy and Casanova, 2001; Niedergang et al., 2003). ARF6 activity is also required for regulated secretion in adipocytes and neuroendocrine cells (Yang and Mueckler, 1999; Vitale et al., 2002). These observations point to a crucial role for ARF6 in plasma membrane and cortical actin remodeling through the regulation of membrane recycling to specialized regions of the plasma membrane. However, our understanding of the mechanism of ARF6 membrane remodeling is still limited and awaits the identification of new effector pathways.

The delivery of membrane vesicles to spatially restricted areas of the plasma membrane is a multi-step process requiring polarized transport, restricted docking and fusion of vesicles to specific plasma membrane sites (for review see Finger and Novick, 1998). Recently, an eight-subunit complex termed the exocyst complex has been shown to mediate the vectorial targeting of secretory vesicles to sites of membrane insertion in yeast (TerBush and Novick, 1995). The exocyst complex is conserved in mammals where it plays a role in vesicle delivery from a post-Golgi compartment to specific plasma membrane domains of epithelial and neuronal cells (Grindstaff et al., 1998; Hazuka et al., 1999; Lipschutz et al., 2000; Vega and Hsu, 2001; Yeaman et al., 2001). Although little is known about the regulation of exocyst complex function, interactions between small GTP binding proteins and exocyst complex subunits have been reported (for review see Lipschutz and Mostov, 2002). These interactions suggest a potential connection between signaling and modulation of polarized membrane growth by the exocyst complex. In this study, we identify the exocyst complex as a novel effector for ARF6, mediating endocytic membrane recycling to dynamic regions of the plasma membrane.

Results

Sec10 interacts with GTP-ARF6

We used a yeast two-hybrid screen in order to identify new ARF6 GTP-binding effector proteins. 2,000,000 clones of a human placenta cDNA library were screened with the constitutively activated ARF6 mutant ARF6-Q67L as a bait. 43 clones were isolated that associated specifically with ARF6-Q67L compared with negative controls (vector, nucleotide-binding–defective ARF6-T27N, and lamin). Among these, two clones corresponded to the carboxy-terminal region of the human Sec10 subunit (aa 378–708) of the exocyst complex (Guo et al., 1997, 1999a). Fig. 1 A documents the two-hybrid interaction of Sec10/378–708 (hereafter called Sec10CTer) with the activated mutant form ARF6-Q67L; no such interaction was detected with wild-type and nucleotide-binding–defective ARF6-T27N. In addition, there was also no interaction of Sec10CTer with the activated form of Rac1, RhoG, RhoB, Cdc42, or Rab6 (unpublished data). Further deletion of the amino- or carboxy-terminal end of Sec10CTer (Sec10/489–708 and Sec10/378–605, respectively) prevented two-hybrid association with ARF6-Q67L (unpublished data). Introduction of two mutations in the ARF6 effector region known to interfere with function (ARF6-Q37E/S38I/Q67L; Al-Awar et al., 2000) abolished the interaction with Sec10CTer, as did deletion of the 13 most amino-terminal residues of ARF6 (unpublished data).

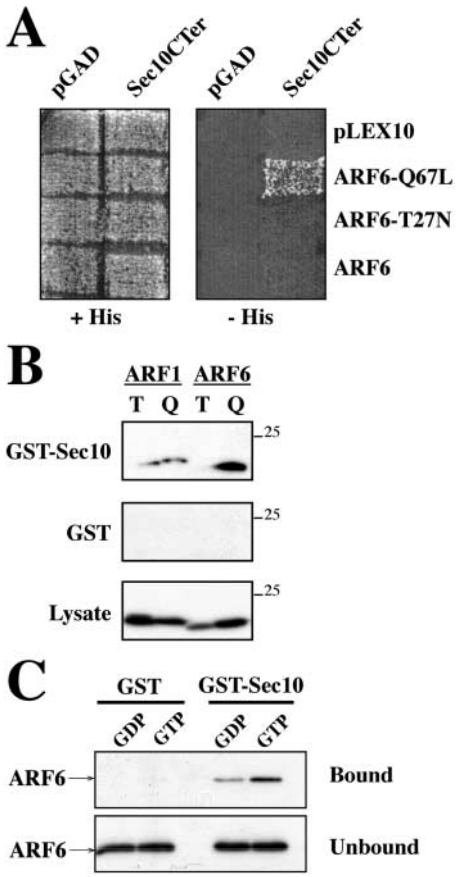

Figure 1. **Interaction of GTP-ARF6 with Sec10.** (A) The indicated ARF6 variants as fusions to the LexA DNA-binding domain were expressed in the L40 yeast two-hybrid reporter strain together with the carboxy-terminal region of human Sec10 (Sec10CTer; aa 378–708 expressed as a fusion to the Gal4 transcriptional activation domain). Growth on medium lacking histidine indicates a positive two-hybrid interaction. (B) To assess the interaction of ARF6 with Sec10, HeLa cells were transfected with carboxy-terminally HA-tagged ARF6 or ARF1 variants, and cell extracts were incubated with Sec10 expressed and purified from *Escherichia coli* as a fusion to GST, or with GST as a control. Complexes were immobilized on glutathione-Sepharose, extensively washed, and separated by SDS-PAGE together with aliquots of total lysates. Detection of bound protein was performed by immunoblotting with anti-HA–tagged mAb. ARF1T, ARF1-T31N; ARF1Q, ARF1-Q71L; ARF6T, ARF6-T27N; ARF6Q, ARF6-Q67L. (C) Beads loaded with GST or GST-Sec10 were incubated with recombinant ARF6 loaded with GDP or GTP. Beads were recovered and bound proteins were eluted. 10% of bound material (top) together with 1% of unbound material (bottom) was immunoblotted with anti-ARF6. One representative experiment out of three is shown. Molecular masses are in kD.

All together, these observations are indicative of effector-domain and amino-terminal helix-dependent interactions of GTP-ARF6 with Sec10. Our attempts to coimmunoprecipitate endogenous or overexpressed Sec10 with activated ARF6 failed, suggesting that the ARF6–Sec10 complex is transient or unstable in the conditions used for immunoprecipitation. However, we could observe ARF6–Sec10 interaction using recombinant GST-tagged Sec10 in two different ways. First, by incubating GST-Sec10 with lysates of cells overexpressing ARF1 and ARF6 variants. The GST pull-down assay showed a specific association of HA-tagged

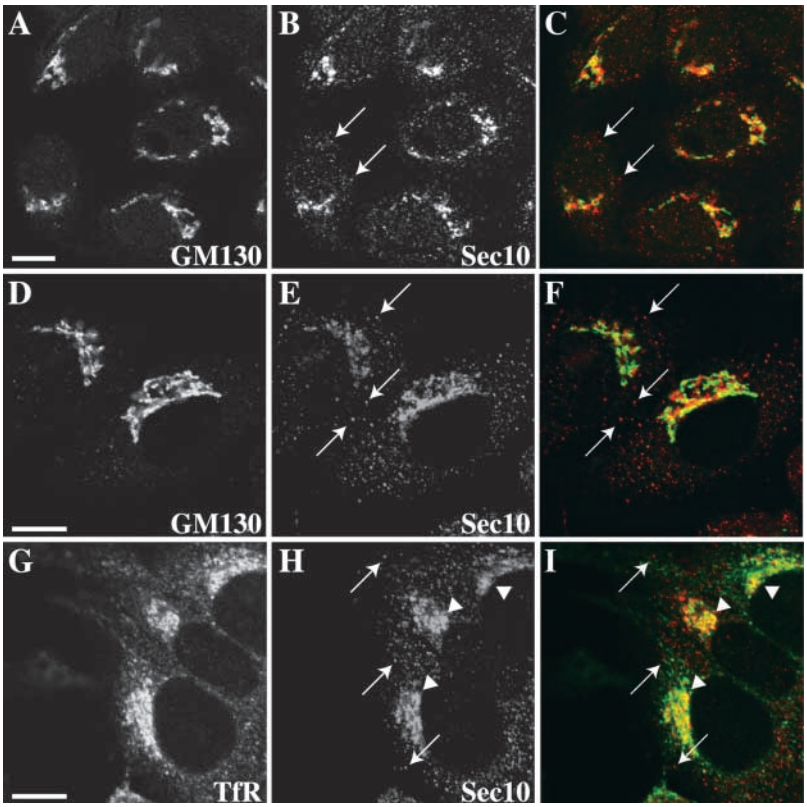

Figure 2. **Immunofluorescence localization of Sec10 to the perinuclear region of MDCK and NRK cells.** The localization of Sec10 (B, E, and H) and the Golgi marker GM130 protein (A and D), or the RE marker TfR (G), was compared on single optical section by confocal immunofluorescence microscopy in subconfluent MDCK cells (A–C) and in NRK cells (D–I) grown on coverslips. To detect Sec10, cells were labeled with pAbs recognizing an amino-terminal peptide derived from Sec10 (aa 6–20). (C, F, and I) Merged images showing Sec10 in red and GM130 (C and F) or TfR (I) in green depict colocalization in yellow. Sec10 is mostly found at the perinuclear region of the cells, where its distribution partially overlaps with the Golgi marker GM130 (C and F) and the RE marker TfR (I). Some Sec10-positive structures are also visible at the cell periphery (arrows). Arrowheads in H and I depict colocalization of Sec10 and TfR in the perinuclear RE. Bars, 10 μm.

ARF6-Q67L, but not ARF6-T27N with Sec10 (Fig. 1 B). In contrast, both mutant forms of ARF1 showed only a weak interaction with GST-Sec10. To further confirm the nucleotide specificity of the ARF6–Sec10 interaction, GST-Sec10 was incubated with purified recombinant ARF6 loaded either with GTP or GDP as described in the Materials and methods section. The data clearly demonstrated a direct and preferential interaction of GTP-ARF6 with Sec10 as compared with GDP-ARF6 (Fig. 1 C, top). Therefore, we conclude that the Sec10 subunit of the exocyst complex is able to interact preferentially with the activated form of the small GTP-binding protein ARF6.

Sec10 localizes to perinuclear secretory and endocytic recycling compartments

To determine the intracellular distribution of Sec10, we raised pAbs against an amino-terminal Sec10 peptide. Consistent with the predicted mol wt of mammalian Sec10 (Guo et al., 1997), these antibodies detected an ~77-kD single band on immunoblot of normal rat kidney (NRK) and MDCK cell extracts (Fig. S1 A, available at http://www.jcb.org/cgi/content/full/jcb.200305029/DC1) that coimmunoprecipitated with Sec8 (Fig. S1 B).

These antibodies were used to determine the intracellular distribution of Sec10 and the exocyst complex by immunofluorescence and immuno-EM. In nonpolarized MDCK cells and in NRK cells, Sec10 localization was predominantly perinuclear and partially overlapped with the distribution of the Golgi marker GM130 (Fig. 2, A–C and D–F, respectively). Immuno-EM of nonpolarized MDCK cells and NRK cells revealed localization of endogenous Sec10 to tubulo-vesicular structures close to Golgi cisternae and corresponding presumably to the TGN (Fig. 3, A and D, respectively; arrows). These observations are in agreement with reported association of the Sec6, Sec8, and Exo70 exocyst subunits with the TGN (Vega and Hsu, 2001; Yeaman et al., 2001). Interestingly, Sec10 was also detected in scattered vesicular structures visible by immunofluorescence microscopy in MDCK (Fig. 2 B, arrows) and in NRK cells (Fig. 2, E and H; arrows). By immuno-EM, some of the Sec10-positive structures appeared as peripheral vesicles closely apposed to endosomal organelles (Fig. 3, B–D; asterisks) with a characteristic vacuolar region and few intraluminal vesicles (Fig. 3, B and C, MDCK cells; Fig. 3 D, NRK cells, arrowheads point to Sec10 labeling). As shown in Fig. 3 C, these vesicular elements are likely to correspond to endosomal buds. The localization of Sec10 to endocytic compartments was studied by double-labeling immunofluorescence microscopy analysis of NRK cells with a combination of anti-TfR mAb and anti-Sec10 antibodies. A significant overlap of Sec10 and TfRs was observed in perinuclear compartments (Fig. 2, G–I; arrowheads). To ascertain the presence of Sec10 in recycling endocytic compartments, we used whole-mount immuno-EM as initially described by Stoorvogel et al. (1996). NRK cells were incubated with HRP-conjugated transferrin (Tf) to fill the entire recycling pathway, and were processed for whole-mount immuno-EM as described in the Materials and methods section. Anti-Sec10 antibodies decorated vesicular endosomal structures and appeared enriched in endosomal buds (Fig. 3, E and F; arrows), some of which were also labeled for TfRs (Fig. 3 F, arrow). Based on these data, we conclude that beside its previously known localization to the TGN and to some

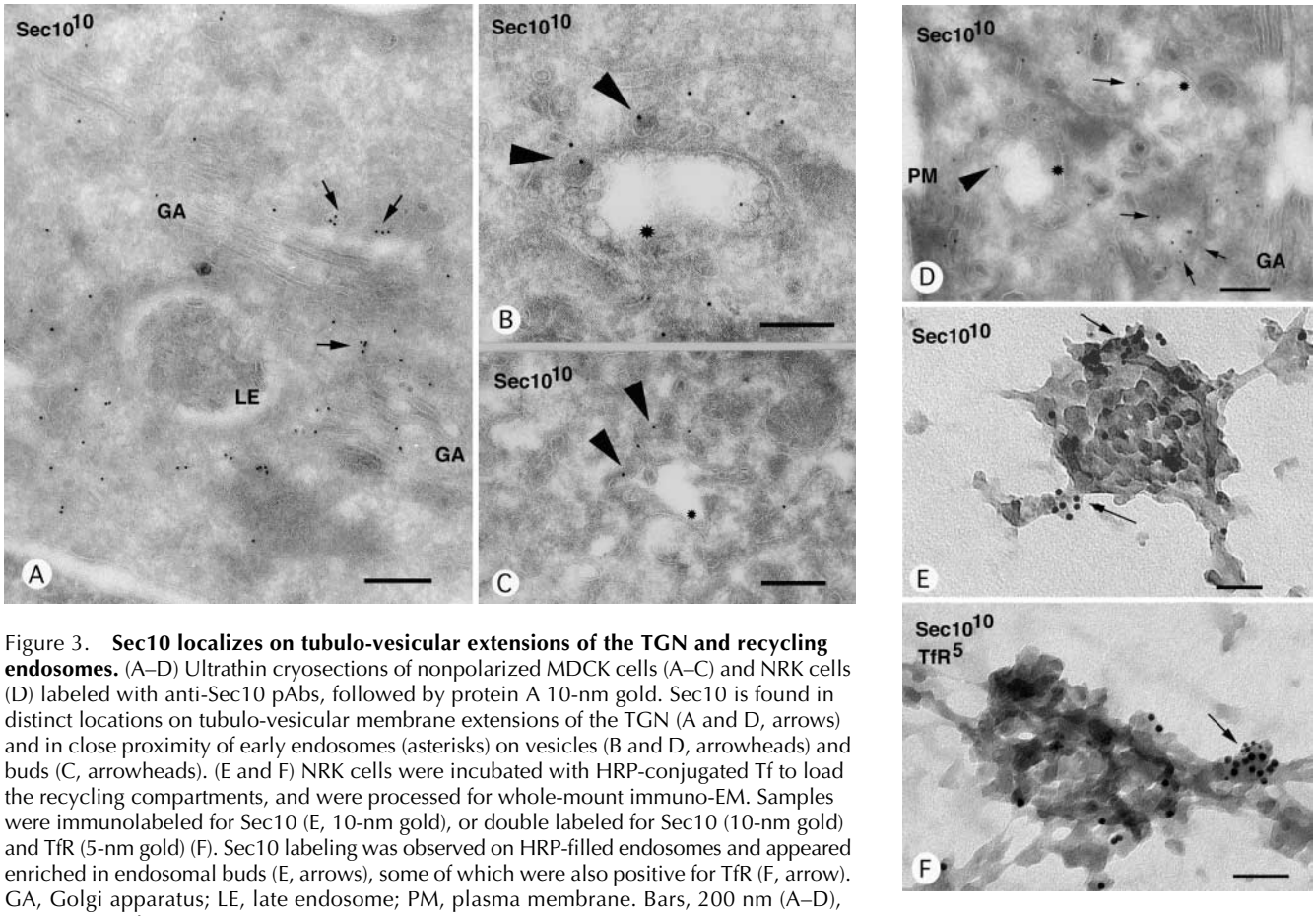

Figure 3. **Sec10 localizes on tubulo-vesicular extensions of the TGN and recycling endosomes.** (A–D) Ultrathin cryosections of nonpolarized MDCK cells (A–C) and NRK cells (D) labeled with anti-Sec10 pAbs, followed by protein A 10-nm gold. Sec10 is found in distinct locations on tubulo-vesicular membrane extensions of the TGN (A and D, arrows) and in close proximity of early endosomes (asterisks) on vesicles (B and D, arrowheads) and buds (C, arrowheads). (E and F) NRK cells were incubated with HRP-conjugated Tf to load the recycling compartments, and were processed for whole-mount immuno-EM. Samples were immunolabeled for Sec10 (E, 10-nm gold), or double labeled for Sec10 (10-nm gold) and TfR (5-nm gold) (F). Sec10 labeling was observed on HRP-filled endosomes and appeared enriched in endosomal buds (E, arrows), some of which were also positive for TfR (F, arrow). GA, Golgi apparatus; LE, late endosome; PM, plasma membrane. Bars, 200 nm (A–D), 75 nm (E), and 60 nm (F).

specialized sites at the plasma membrane (Grindstaff et al., 1998; Hazuka et al., 1999; Lipschutz et al., 2000; Vega and Hsu, 2001), the exocyst complex is also present in the recycling endocytic pathway.

Interfering with Sec10–exocyst complex function affects trafficking in the recycling pathway

Deletion of the carboxy-terminal region of yeast or mammalian Sec10 creates a dominant-negative form that inhibits exocyst complex activity (Roth et al., 1998; Vega and Hsu, 2001). Based on these observations, we fused aa 1–537 of human Sec10 at the carboxy-terminal end of GFP (GFP-Sec10NTer), and expressed this construct in NRK cells to assess its effect on the recycling pathway. Perinuclear REs labeled with TfRs underwent a striking reorganization in NRK cells expressing GFP-Sec10NTer. TfRs were found in an extensive network of long and thin tubular extensions of the perinuclear region (Fig. 4 B, arrows). Tubules were observed in ~30% of Sec10NTer-expressing cells and never seen in nontransfected cells (Fig. 4 B, cell at bottom right) or in cells expressing full-length Sec10 (unpublished data). Fluorescent Tf internalized for 30 min was also found in these tubular structures in Sec10NTer-expressing NRK cells (Fig. 4 D, arrows). Expression of GFP-Sec10NTer had no effect on the morphology of the TGN (Fig. 4 F, labeled with TGN38), the Golgi apparatus (labeled with GM130; unpublished data), or early endosomes (stained with EEA1; unpublished data).

These results suggested that the exocyst complex has a specific function in the recycling pathway. This issue was addressed by transfecting HeLa cells with a 21-bp double-stranded small interfering RNA (siRNA) designed from the sequence encoding the human Sec5 exocyst complex subunit, which knocked down Sec5 to undetectable level after 72 h (Fig. 5 A, left). By phase-contrast microscopy, Sec5-depleted cells appeared rounder than mock-transfected cells, but growth of both cell populations was comparable (unpublished data). After 72 h of treatment, cells were allowed to internalize Alexa® 488–labeled Tf for 30 min, and FACS® analysis was used to measure the kinetics of Tf recycling (Fig. 5 B). Depletion of Sec5 levels correlated with a significant and reproducible diminution of Tf release as compared with control mock-transfected cells. All together, these observations are consistent with a role for the exocyst complex in the recycling pathway.

GTP-ARF6 promotes the redistribution of the exocyst complex from the perinuclear region to the plasma membrane

To investigate the role of ARF6 in exocyst complex function in the recycling pathway, we first examined the effect of HA-tagged dominant-inhibitory ARF6-T27N on the distribution of the complex visualized with anti-Sec10 antibodies. As shown in Fig. 6 (A and B), the distribution of Sec10 in the perinuclear region was not affected in MDCK cells ex-

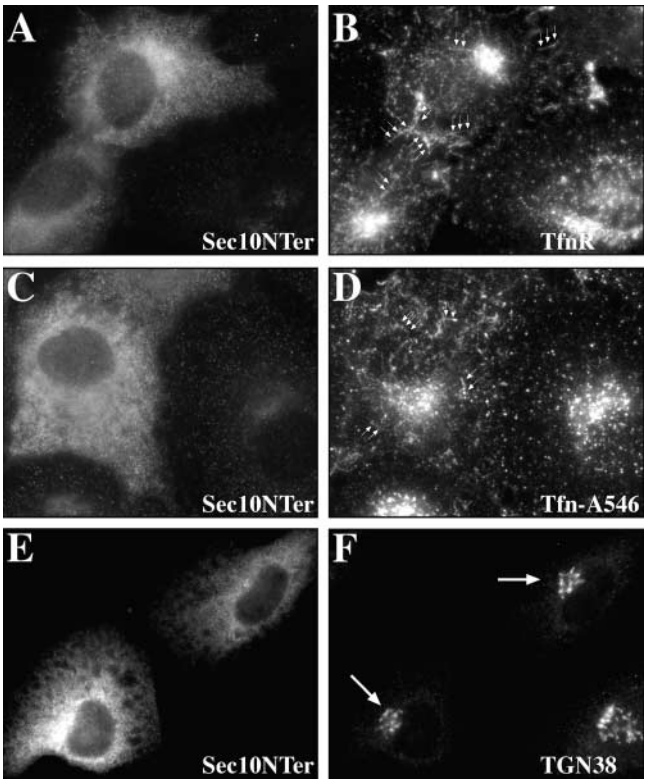

Figure 4. **Morphological alterations of recycling endosomes in cells expressing Sec10NTer.** (A and B) NRK cells were transiently transfected with GFP-tagged Sec10NTer. 24 h after transfection, cells were fixed and stained with anti-TfR mAb. GFP-Sec10NTer is shown in A, TfR is shown in B. Arrows in B depict beaded tubular structures containing TfRs. (C and D) After transfection, NRK cells were incubated with Alexa® 546–labeled Tf at 37°C for 20 min. The cells were washed, fixed, and observed by confocal microscopy. GFP-Sec10NTer is shown in C. Tf is depicted in D. Arrows in D depict Tf accumulation in beaded tubular structures that are induced by Sec10NTer expression. (E and F) Cells transfected with GFP-Sec10NTer were stained for TGN38 (F). GFP-Sec10NTer is shown in E. Arrows in F indicate normal TGN structures.

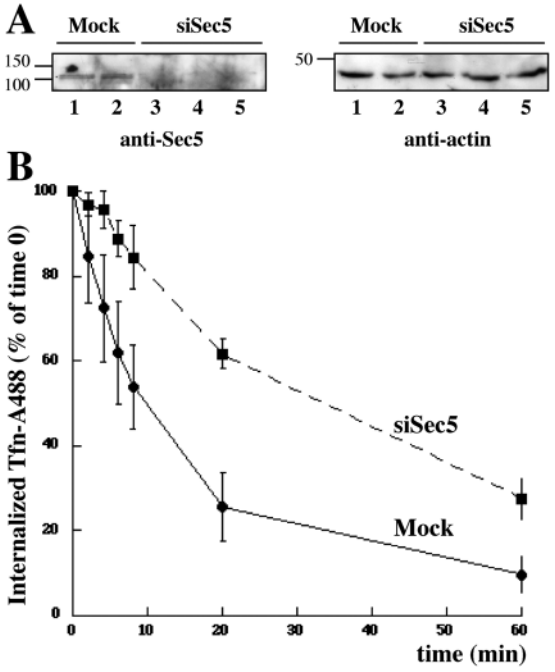

Figure 5. **Kinetics of Tf recycling in control and Sec5 siRNA-treated HeLa cells.** (A) Equal protein loadings of lysates of either mock-transfected cells (two independent experiments) or cells transfected with siRNA directed against the exocyst Sec5 subunit (three independent experiments) were separated by SDS-PAGE and analyzed by immunoblotting with anti-Sec5 antibodies (left), or anti-actin antibodies as a control (right). 72 h of treatment with siRNA causes depletion in the Sec5 subunit. (B) HeLa cells were transfected with Sec5 siRNA or were mock transfected. 72 h after transfection, cells were detached and incubated in medium containing 50 nM Alexa® 488–Tf for 30 min at 37°C. Recycling of Tf was then measured by FACS® as described in the Materials and methods section. The mean Alexa® 488–Tf fluorescence was calculated for each time point measured in duplicate, and expressed as a percentage of the fluorescence obtained after 30 min of internalization (zero time point). The plots represent the mean ± SEM of three independent experiments. Cells depleted in the Sec5 subunit recycle Tf with reduced kinetics.

pressing ARF6-T27N, indicating that steady-state association of the exocyst complex to perinuclear compartments does not require GTP-ARF6. Next, the effect of the constitutively activated ARF6-Q67L mutant was investigated. As reported in D'Souza-Schorey et al. (1998), a significant fraction of ARF6-Q67L was found at the surface of MDCK cells that exhibited long membrane extensions and ruffles (Fig. 6, D, F, and H, and see below). As shown in Fig. 6 C and D, loss of perinuclear Sec10 staining was observed in ARF6-Q67L-expressing cells. This effect was better visualized in cells expressing medium to high levels of GTP-ARF6. In contrast, neither the distribution of GM130 nor that of TGN38 was affected by expression of ARF6-Q67L even at high levels (Fig. 6; E and F and G and H, respectively). Similar observations were made in HeLa and NRK cells (unpublished data).

Disappearance of Sec10 from the perinuclear region of cells overexpressing ARF6-Q67L suggested that the complex could be displaced from perinuclear compartments to the cell periphery as a result of a Sec10 interaction with GTP-ARF6 at the plasma membrane. However, immunofluorescence labeling did not reveal plasma membrane staining of Sec10 in ARF6-Q67L–expressing cells (Fig. 6, C and D). It is of note that a series of anti-Sec6/8 mAbs has been recently characterized showing mutually exclusive staining of the TGN or the plasma membrane (Yeaman et al., 2001), suggesting the existence of distinct exocyst complex conformations. Therefore, it is possible that epitope masking may have prevented Sec10 recognition at the plasma membrane with anti-Sec10 peptide antibodies in the immunofluorescence analyses described above. As Sec10 labeling in close proximity to the plasma membrane was detected by immuno-EM (Fig. 3, and unpublished data), we assessed the localization of Sec10 in MDCK Tet-Off™ cells stably expressing HA-tagged ARF6-Q67L at EM level. Two clones showing no detectable expression of ARF6-Q67L in the presence of doxycycline, but an approximate twofold overexpression compared with endogenous ARF6 upon removal of the drug, were selected and gave similar results (Fig. S2 A, available at http://www.jcb.org/cgi/content/full/jcb.200305029/DC1; unpublished data). Phase-contrast analysis of the clones grown in

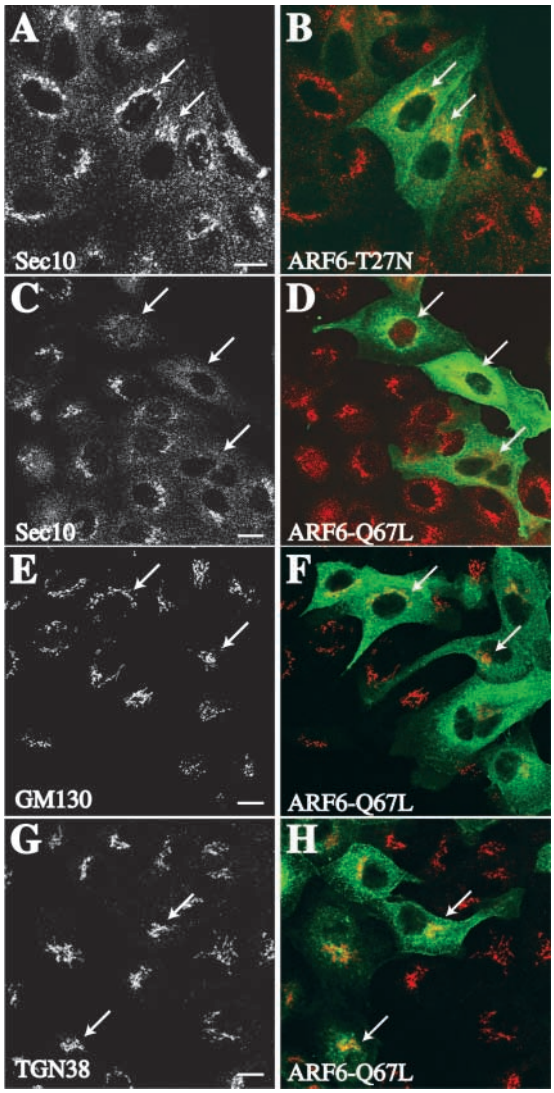

Figure 6. **Selective loss of Sec10 from perinuclear compartments by expression of activated ARF6.** Subconfluent MDCK cells grown on coverslips were transiently transfected with constructs encoding HA-tagged dominant inhibitory ARF6-T27N (A and B), or constitutively activated ARF6-Q67L (C–H). (A and B) Cells expressing ARF6-T27N were double labeled with anti-HA (B, green) and anti-Sec10 (A, red in B). ARF6-T27N has no effect on the perinuclear localization of Sec10 (arrows). (C and D) Cells expressing ARF6-Q67L were double labeled with anti-HA (D, green) and anti-Sec10 (C, red in D). ARF6-Q67L expression induces a disappearance of Sec10 from perinuclear compartments (arrows). (E–H) Cells expressing ARF6-Q67L were double labeled with anti-HA (F and H, green) and anti-GM130 (E, red in F), or with TGN38 (G, red in H). ARF6-Q67L expression has no effect on the distribution of Golgi marker GM130 or TGN marker TGN38 proteins (arrows). Bars, 10 μm.

the absence of doxycycline revealed that expression of GTP-ARF6 had a strong effect on the morphology of MDCK cells, forming loose colonies as compared with compact colonies observed when the clones were grown in the presence of the drug (Fig. S2, compare B with C). Overexpression of GTP-ARF6 triggered the formation of extensive membrane ruffles and of thin, long membrane protrusions (several tens of μm in length) with fan-shaped ends (Fig. S2 C). At the EM level, cells expressing GTP-ARF6 exhibited extensive folds and extensions that appeared as membrane-enclosed structures with an electrolucent lumen in cross section (Fig. S2, compare D–F with Fig. 7, asterisks). Immunogold labeling revealed that Sec10 accumulated along the plasma membrane folds (Fig. 7, arrows), as well as with plasma membrane invaginations and tubulo-vesicular structures in close proximity to the ruffled plasma membrane (Fig. 7, arrowheads), whereas no such accumulations were visible in doxycycline-treated cells (Fig. S2, D and E). All together, these data suggest that the exocyst complex, by interacting with GTP-ARF6, is recruited to the plasma membrane in membrane extensions that form on activation of ARF6.

Inhibition of GTP-ARF6–induced membrane spreading by dominant-negative Sec10

On the basis of the above findings, we postulated that if the exocyst complex was required downstream of ARF6 for post-endocytic recycling, coexpression of the inhibitory Sec10 mutant together with GTP-ARF6 should affect ARF6-induced membrane recycling and inhibit subsequent plasma membrane extension. Expression of ARF-Q67L in NRK cells has been shown to induce cell spreading (Song et al., 1998). Therefore, we expressed ARF6-Q67L alone or in combination with inhibitory Sec10NTer in NRK cells, and measured the projected cell area as described in the Materials and Methods section. Confirming previous findings (Song et al., 1998), expression of ARF6-Q67L resulted in a statistically significant increase of cell area when compared with GFP-expressing control cells (Fig. 8, compare A with B; see quantification of cell area in D). In contrast, coexpression of activated ARF6 with dominant-negative Sec10NTer led to a significant reduction in cell area as a result of the inhibition of cell spreading (Fig. 8, C and D). Reduction of cell area was also observable in cells expressing Sec10NTer alone (Fig. 8 D). The Sec10NTer construct is unlikely to exert its inhibitory effect by titrating GTP-ARF6, as Sec10NTer retains only the first 159 amino acids of the ARF6-binding domain, insufficient to support ARF6 binding by yeast two-hybrid. Furthermore, expression of GFP-tagged full-length Sec10 did not inhibit cell spreading (unpublished data). Based on these observations, we conclude that the activity of the exocyst is required for ARF6-induced membrane recycling from the RE during cell spreading, and therefore, that the exocyst serves as a downstream ARF6 effector complex in post-endocytic recycling.

Discussion

In this paper, we identify a novel mechanism by which GTP-bound ARF6 promotes membrane recycling toward specialized plasma membrane regions: ARF6 recruits the exocyst complex to sites of plasma membrane growth.

We report that a domain comprising the last 330 residues of Sec10 interacts with ARF6 by a two-hybrid screen and in pull-down assays. This association is direct, and occurs preferentially with activated GTP-ARF6 (Fig. 1). The association of GTP-ARF6 with Sec10 is reminiscent of interactions reported recently in yeast and mammalian cells between the exocyst subunits and several members of the Rab, Rho, and Ral small GTP-binding protein subfamilies (for review see Lipschutz

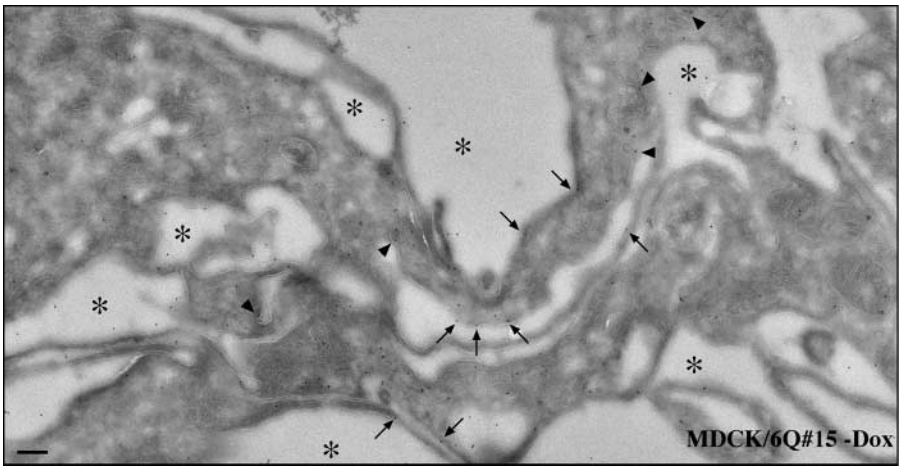

Figure 7. **Localization of Sec10 in dynamic regions of the plasma membrane in GTP-ARF6–expressing cells.** Inducible expression of HA-tagged ARF6-Q67L in MDCK cells was established using the Tet-Off™ system. MDCK cells (clone 15) were cultured in doxycycline-free (−Dox) medium for 48 h to induce ARF6-Q67L expression (Fig. S2, available at http://www.jcb.org/cgi/content/full/jcb.200305029/DC1). Ultrathin cryosections were labeled with anti-Sec10 pAbs, followed by protein A 10-nm gold. In MDCK cells expressing ARF6-Q67L, the plasma membrane exhibited extensive membrane folds and extensions appearing as electroluescent structures (asterisks). Sec10 is detected along plasma membrane folds (arrows) and in membrane invaginations and tubulo-vesicular structures in close proximity to the ruffled plasma membrane (arrowheads). Bar, 200 nm.

and Mostov, 2002; Novick and Guo, 2002). In yeast, the exocyst complex acts presumably by targeting secretory vesicles to sites of exocytosis (Finger and Novick, 1998). Recruitment of Sec15p to secretory vesicles requires its interaction with GTP-Sec4p, a Rab protein functioning in Golgi to plasma membrane transport in yeast (Finger et al., 1998; Guo et al., 1999b). At a later stage on the secretory pathway, interaction of Sec3p with GTP-Cdc42p and GTP-Rho1p, two Rho proteins essential for cell polarity establishment and maintenance, is probably required to direct exocytosis to the bud (Grote et al., 2000; Guo et al., 2001; Zhang et al., 2001). In mammalian cells, Sec5 interacts with GTP-Ral (Moskalenko et al., 2002), which may regulate complex assembly (Moskalenko et al., 2002), whereas interaction of Exo70 with the Rho protein TC10 has recently been implicated in trafficking of Glut4 to the plasma membrane (Inoue et al., 2003). The mammalian exocyst complex is found at specialized sites of the plasma membrane along the axon and in the growth cone of neuronal cells, as well as at epithelial cell–cell contacts (Grindstaff et al., 1998; Hazuka et al., 1999; Lipschutz et al., 2000).

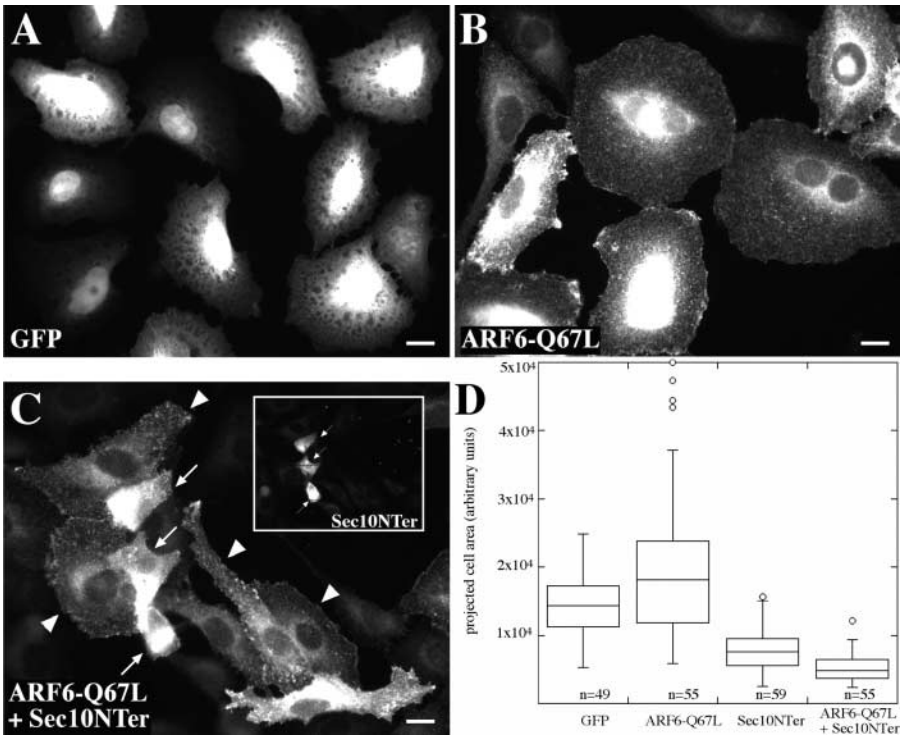

Figure 8. **Expression of the dominant-inhibitory Sec10 amino-terminal domain inhibits ARF6-Q67L–induced spreading of NRK cells.** NRK cells grown on glass coverslips were transiently transfected with GFP (A), HA-tagged ARF6-Q67L (B), or HA-tagged ARF6-Q67L and GFP-tagged Sec10NTer (aa 1–537). (C) Cells were fixed and processed for immunofluorescence labeling with anti-HA–tagged mAb to detect ARF6-Q67L (B and C). A and the inset in C show the fluorescence signal of GFP (A) or GFP-tagged Sec10NTer (C, inset). Arrows in C (and inset) depict cells expressing both ARF6-Q67L and Sec10NTer, whereas cells labeled with arrowheads showed no detectable expression of Sec10NTer and expressed only ARF6-Q67L. (D) Box plot distribution of projected area of cells expressing GFP, ARF6-Q67L, Sec10NTer, or ARF6-Q67L together with Sec10NTer. Cell pixel area was determined with MetaMorph®. The number of cells in each data set is presented below each distribution. The top line of each box represents the third quartile, the middle line the median, and the bottom line the first quartile. Circles indicate outliers. Statistical analysis (*t* test) revealed significant difference between GFP and ARF6-Q67L–expressing cell populations ($P < 0.001$), as well as between populations of cells expressing ARF6-Q67L alone, or in combination with Sec10NTer ($P < 0.001$). Bars, 10 μm.

An intracellular pool of the complex is also detected on the TGN (Vega and Hsu, 2001; Yeaman et al., 2001; Fig. 3, A and D). Interestingly, expression of dominant-inhibitory Sec10 and Sec8 blocks neurite outgrowth in PC12 cells and trafficking to the basolateral membrane in MDCK cells, respectively (Lipschutz et al., 2000; Vega and Hsu, 2001). In addition, Sec10 overexpression stimulates tubule formation in an in vitro model of kidney tubulogenesis (Yeaman et al., 2001). All together, these results support the idea that the exocyst complex is required for transport between the TGN and sites of plasma membrane growth. Our data indicate that the perinuclear distribution of the exocyst complex in mammalian cells is not restricted to the TGN (Vega and Hsu, 2001; Yeaman et al., 2001), but extends into REs. Here, we demonstrate that TfR-containing endocytic buds that are abundant on REs (Stoorvogel et al., 1996) carry endogenous Sec10. This is consistent with data showing that Exo70 and Sec8 exocyst subunits are associated with TfR-positive REs in MDCK cells (Folsch et al., 2003). However, it is unlikely that the recruitment of Sec10 to the RE requires GTP-bound ARF6, as perinuclear Sec10 localization is not affected by dominant-inhibitory ARF6 that lowers GTP-ARF6 level. Rather, our observations indicate that GTP-ARF6, which accumulates at the plasma membrane (D'Souza-Schorey et al., 1998; Frank et al., 1998; Franco et al., 1999; Vitale et al., 2002), triggers the localization of Sec10, and the exocyst complex, to plasma membrane protrusions and invaginations that form upon ARF6 activation (Fig. 7).

Depending on the cell types, ARF6 has been shown to control the recycling of proteins endocytosed through the clathrin-dependent pathway (D'Souza-Schorey et al., 1995, 1998), or to transport proteins that are endocytosed independently of clathrin (Radhakrishna and Donaldson, 1997; Naslavsky et al., 2003). Although it has not been clarified whether these pathways intersect and whether recycling materials follow a common route back to the plasma membrane, ARF6 activity has consistently been associated with the formation of actin-based plasma membrane protrusions (Song et al., 1998; Franco et al., 1999; Radhakrishna et al., 1999; Palacios et al., 2001). Accordingly, ARF6 is implicated in the regulation of cellular processes requiring a transient mechanism to deliver membranes to regions of the cell surface reorganization. A common feature of these processes (including membrane ruffling, cell spreading, cell motility, and phagocytosis; Song et al., 1998; Zhang et al., 1998; Radhakrishna et al., 1999; Palacios et al., 2001; Santy and Casanova, 2001; Niedergang et al., 2003) is that polarized endocytic recycling contributes to cellular polarization. Directional recycling of TfRs and integrins to the leading edge has been reported during cell spreading and motility in fibroblasts (Hopkins et al., 1994; Pierini et al., 2000; Laukaitis et al., 2001; Roberts et al., 2001). Similarly, recycling endocytic vesicles positive for VAMP3 insert at the site of pseudopod extension during phagocytosis in macrophages, in a process that is under ARF6 control (Bajno et al., 2000; Niedergang et al., 2003). Here, we found that spreading of ARF6-Q67L–expressing NRK cells is strongly inhibited by coexpression of dominant-inhibitory Sec10. This observation, together with the reported inhibition of NRK and HeLa cell spreading upon inhibition of ARF6 function (Radhakrishna and Donaldson, 1997; Song et al., 1998), suggests that membrane delivery from internal endocytic reservoirs is a major player during cell spreading in a process that involves the ARF6/exocyst complex machinery controlling membrane insertion at the plasma membrane.

Therefore, we favor a model that considers that local ARF6 activation at the plasma membrane is required for polarized membrane recycling and insertion through interaction of GTP-ARF6 with the vesicle-tethering exocyst complex. According to this model, interfering with exocyst complex activity is expected to impair docking of recycling transport intermediates with the plasma membrane. Indeed, we observed a partial inhibition of Tf recycling in Sec5-depleted cells, consistent with the observation that only a fraction of Tf recycles to the plasma membrane through REs (Sheff et al., 1999). In addition, the observation that dominant inhibition of Sec10 function triggers the formation of an extensive endocytic tubular network is also consistent with an essential role of the exocyst complex in endocytic recycling. Analogous to findings in yeast where inhibition of Sec10p leads to intracellular membrane accumulation (Roth et al., 1998), we believe that this morphological change is produced by interfering with the docking of recycling transport intermediates with the plasma membrane. Although our findings bring novel insights as to how ARF6 may control delivery of recycling vesicles, they do not explain how the exocyst complex can operate simultaneously in post-Golgi and endocytic recycling pathways without mixing. One possibility is that specificity is provided earlier when the exocyst complex is recruited to donor compartments or vesicles.

In yeast, Sec4p acts as a bridge between the exocyst and post-Golgi transport vesicles by interacting with Sec15p (Finger et al., 1998; Guo et al., 1999b). Interestingly, two sec15 genes have been identified in mammalian cells encoding two related proteins (Sec15A and Sec15B; Kee et al., 1997; Brymora et al., 2001). These observations suggest the existence of at least two forms of the exocyst complex that may interact with specific Rab GTPases on distinct membranes. Directionality and specificity may also be achieved by polarized vesicle transport. Recently, it has been shown that a subset of microtubules could serve as a track to facilitate export from the RE to the cell surface (Lin et al., 2002), and a direct association of the exocyst complex with microtubules has been reported (Vega and Hsu, 2001). Future experiments should define the function of ARF6 in coordinating these various mechanisms that target post-endocytic recycling to sites of membrane growth during cell polarization.

Materials and methods

Cell culture, antibodies, and reagents

MDCK I cells and NRK cells were cultured in DME supplemented with 10% FBS, penicillin, and streptomycin. pAbs against Sec10 were generated against a synthetic peptide (ELFEEPFVADEYIER) corresponding to aa 6–20 of human Sec10. Anti-Sec10 antibodies from rabbit sera were purified by affinity chromatography on the Sec10 peptide immobilized on a HiTrap™ NHS-activated HP column (Amersham Biosciences). Rat mAb against HA tag (clone 3F10) was purchased from Roche. Anti-GM130 (clone 35) and anti–rat Sec8 (clone 14) mouse mAbs were purchased from BD Biosciences. Anti–human TfR (intracellular domain) mouse mAb (clone H68.4) was obtained from Zymed Laboratories. Mouse mAb against

rat Sec6 (clone 9H5) was purchased from StressGen Biotechnologies. Rabbit pAbs against ARF6, and TGN38 were provided by Drs. V.W. Hsu (Brigham and Women's Hospital, Boston, MA) and G. Banting (University of Bristol, UK), respectively. Mouse mAb against Exo70 was a gift of Dr. S.-C. Hsu (Rutgers University, Piscataway, NJ). Anti-Sec5 antibodies were generated by immunization of rabbits with the Ral-binding domain of Sec5 fused to GST (Moskalenko et al., 2003). Cy2- and Cy3-conjugated secondary antibodies were purchased from Jackson ImmunoResearch Laboratories. Alexa®-conjugated Tf was purchased from Molecular Probes, Inc.

Yeast two-hybrid screening

Two-hybrid screening was performed using a mating protocol with L40 and Y187 yeast strains, using a fusion of LexA with ARF6-Q67L as a bait and a human placenta random-primed cDNA library fused to the Gal4 activation domain, using standard procedures (Vojtek and Hollenberg, 1995).

ARF6–Sec10 binding assays

Sequences encoding full-length Sec10 or its amino-terminal region (Sec10NTer; aa 378–708) were subcloned into pGEX4T1 at the carboxy terminus of GST and transformed in *E. coli* BL21(DE3) strain. Expression was induced with 0.5 mM isopropyl β-D-thiogalactopyranoside for 5 h at 25°C. The fusion protein was purified by affinity chromatography on glutathione-Sepharose beads (Amersham Biosciences). After elution with glutathione, the purified protein was dialyzed against 20 mM Tris, pH 7.4, 100 mM NaCl, 2 mM EDTA, 2 mM β-mercaptoethanol, and 10% glycerol, and was stored at −80°C.

For the in vitro binding assay, recombinant ARF6 (rARF6) was purified from *E. coli* mostly as a GTP-bound form as described previously (Chavrier and Franco, 2001). Loading with GDP was obtained by the addition of 2 mM EDTA (free Mg^{2+} ~1 μM) in the presence of 5 mM excess GDP for 60 min at 25°C, followed by addition of 2 mM $MgCl_2$. In these conditions, ~50% of rARF6 was converted in the GDP-bound form. Separation of the GTP- and GDP-bound forms of ARF6 (5 mg total rARF6) was performed by chromatography on a cation exchange column (Mono S HR5/5; Amersham Biosciences) equilibrated in buffer A (50 mM Tris-HCl, pH 7.5, 1 mM $MgCl_2$, 1 mM DTT, and 10 μM GDP) at a flow rate of 1 ml/min. Elution was performed with a linear gradient of 0–1 M NaCl in buffer A, GTP- and GDP-ARF6 eluting at ~70 mM and 110 mM NaCl, respectively. 8 μM GTP- or GDP-bound rARF6 was incubated together with GST or GST-Sec10, and was bound to glutathione-Sepharose beads (4 μM) for 60 min at 4°C in binding buffer (50 mM Tris-HCl, pH 7.5, 100 mM NaCl, 2 mM $MgCl_2$, 1 mM DTT, and 0.5% Triton X-100) containing 100 μM GDP (GDP-ARF6 binding experiment) or GTP (GTP-ARF6 binding experiment) and 0.5% BSA (wt/vol). Beads were washed twice with binding buffer plus 0.5% BSA and twice with binding buffer. Bound proteins were eluted in SDS sample buffer and separated by SDS-PAGE. rARF6 in the bound (10% of total) and unbound (1% of total) fraction was detected by immunoblotting analysis using anti-ARF6 antibodies.

For the in vivo binding assay, HeLa cells were transfected with plasmids encoding HA-tagged ARF1 and ARF6 variants using the calcium-phosphate method. Cells were lysed 36 h after transfection with 50 mM Tris, pH 7.4, 100 mM NaCl, 1 mM EDTA, 1% Triton X-100, and a cocktail of protease inhibitors (Roche), and centrifuged at 13,000 rpm for 5 min at 4°C. Supernatants were incubated with GST or GST-Sec10 for 30 min at 4°C in the presence of 0.1% BSA, and then glutathione-Sepharose beads were added for 1 h further. Beads were washed three times with 1 ml 50 mM Tris, pH 7.4, 100 mM NaCl, 1 mM EDTA, and 1% Triton X-100. Bound proteins were eluted using SDS sample buffer, and were separated by SDS-PAGE. The presence of ARF on the beads was detected by Western blot analysis using anti-HA antibodies.

Generation of stable MDCK cell lines

cDNAs encoding HA-tagged ARF6-T27N and -Q67L have been described previously (Franco et al., 1999). Tet-Off™ MDCK cells were transfected with FuGENE™ 6 reagent with the cDNA-encoding HA-tagged ARF6-Q67L subcloned in pTRE expression vector (CLONTECH Laboratories, Inc.) and pSPGK-Hygro. Resistant clones were maintained in medium containing 400 μg/ml hygromycin, 200 μg/ml G418, and 1 μg/ml doxycycline. Regulated expression of HA-tagged ARF6-Q67L in resistant clones was assessed by immunoblotting analysis with anti-ARF6 antibodies after 72 h of culture with or without doxycycline. Two clones (named clone 15 and 17) were selected, and gave identical results.

Transient transfection and Tf uptake

Expression plasmid for dominant inhibitory Sec10 (aa 1–537) was generated by PCR from human Sec10 cDNA (a gift of Dr. P. De Camilli, Yale University School of Medicine, New Haven, CT) and by in-frame insertion at the carboxy terminus of E-GFP in the pEGFP-C1 expression vector (CLONTECH Laboratories, Inc.).

For transient transfection, MDCK I cells were trypsinized and resuspended at a density of 2.5×10^7 cells/ml in culture medium supplemented with 15 mM Hepes, pH 7.5. 5×10^6 cells were electroporated in a 0.4-cm cuvette (Equibio) with 20 μg plasmid DNA encoding HA-tagged ARF6-Q67L variants (Franco et al., 1999) with a Gene Pulser II apparatus (950 μF, 240 V; Bio-Rad Laboratories). Cells were usually analyzed 36 h after transfection. NRK cells grown on coverslips were transfected with FuGENE™ 6 reagent (Roche) according to the manufacturer's procedure. For Tf uptake, 30 h after transfection, cells were incubated in internalization medium (DME supplemented with 20 mM Hepes, pH 7.4, and 1% wt/vol BSA) for 30 min at 37°C. Then, cells were incubated in internalization medium containing 10 μg/ml Alexa® 546–conjugated human Tf (Molecular Probes, Inc.) for 30 min. Cells were fixed and processed for immunofluorescence labeling.

Immunofluorescence microscopy

Cells on coverslips were fixed, permeabilized, immunolabeled, and visualized for fluorescence staining as described previously (Guillemot et al., 1997). Optical sections were taken with a confocal microscope (TCS SP2; Leica). For determination of projected cell area, images were analyzed with the Integrated Morphometry Analysis module of MetaMorph® 5.04 software (Universal Imaging Corp.).

Quantification of Tf recycling

HeLa cells were transfected with siRNA duplex (Dharmacon) specific for human Sec5 with Oligofectamine® according to the manufacturer's instruction (Invitrogen; Elbashir et al., 2001; Sec5 siRNA duplex: (Sec5–1), 5′-CGGCAGAAUGGAUGUCUGC-3′; (Sec5–2), 5′-GGUCGGAAAGACAAGGCAGAU-3′). After 72 h, cells were detached in 1% EDTA/PBS and pelleted. Cells were resuspended in internalization medium (DME, 10 mM Hepes, pH 7.4, and 0.1% BSA) supplemented with 50 nM Alexa® 488–labeled human Tf and incubated at 37°C. After 30 min, cells were diluted with cold internalization medium, pelleted, and resuspended in cold internalization medium supplemented with 1.5 μM human holo-Tf. An aliquot of cells was taken and kept on ice (time 0), and the remaining cells were incubated at 37°C. At the indicated time during the recycling period, aliquots of cells were taken, diluted four times in 0.1% BSA/PBS, and kept on ice. All time points were done in duplicate. FACS® analysis was performed using a FACScan™ (Becton Dickinson) measuring Alexa® 488 in FL1. Live cells were selected using a forward scatter/side scatter gate, and data from at least 2×10^3 live cells were acquired. The mean Alexa® 488 fluorescence was calculated as the averaged means of duplicate samples.

Electron microscopy

For immunogold labeling on ultrathin cryosections, cells were fixed with 2% PFA in PBS for 2 h at RT. Fixed cells were processed for ultrathin cryosectioning, and were immunogold labeled (Raposo et al., 1997). Antibodies were visualized with Protein A–gold conjugates (purchased from the Department of Cell Biology, Utrecht University, Utrecht, Netherlands). After staining and embedding with a mixture of uranyl acetate and methylcellulose, sections were viewed at 80 kV with a transmission electron microscope (Philips CM120; FEI Company).

For whole-mount EM, immunogold labeling of Sec10 and TfR on entire NRK cells was performed as described by Stoorvogel et al. (1996) on cells grown for 2 d on formvar-coated gold grids. In brief, after washing with MEM, 20 mM Hepes, pH 7.4, cells were starved for 45 min in the same medium at 37°C and then incubated for 45 min with 50 μg/ml of HRP-conjugated mouse Tf (Pierce Chemical Co.). Cells were rapidly cooled at 4°C and incubated in DAB-H_2O_2–containing buffer in order to fill Tf-containing compartments with DAB polymer that served as an electron-dense marker for endosomes. Soluble cytosolic proteins were removed by permeabilization with saponin, and cells were then fixed with 3% PFA in 0.1 M phosphate buffer, pH 7.4, for 2 h. Immunogold labeling was performed at RT in the presence of saponin and using cold fish gelatin as blocking buffer. After labeling, cells on grids were fixed with 2% glutaraldehyde, rinsed in water, dehydrated in increasing concentrations of ethanol, and critical point dried in a critical point dry apparatus (Balzers). Samples were viewed with a transmission electron microscope (Philips CM120; FEI Company).

Subcellular fractionation, immunoprecipitation, and immunoblotting analysis

For subcellular fractionation, MDCK Tet-Off™ cells from two selected clones stably transfected with HA-tagged ARF6-Q67L (clones 15 and 17)

were cultured in the presence of 1 μg/ml doxycycline (+Dox), or switched to doxycycline-free (−Dox) medium for 72 h. Cells from the different populations (4×10^6 cells from two 10-cm-diam dishes) were washed and scraped in PBS and homogenized in 250 mM sucrose, 3 mM imidazole, pH 7.4, with protease inhibitors by repeated passages through a $25G^{5/8}$ needle. Homogenate was subjected to a 1,000-*g* spin to yield a postnuclear supernatant (PNS). PNS was subjected to a 100,000-*g* spin to yield soluble (S) and pellet (P) fractions. Pellets were resuspended in sample buffer to volumes equal to that of the corresponding supernatants, and equal volumes of P and S fractions were loaded per lane (corresponding to 25 μg total protein from the soluble fraction). For immunoprecipitation analysis, 2×10^6 MDCK cells were lysed in 1% Triton X-100, 150 mM NaCl, 2 mM EDTA, and 30 mM Tris, pH 7.6, with protease inhibitors at 4°C. Lysates were cleared by centrifugation at 13,000 *g* for 10 min at 4°C, and 5 μg affinity-purified rabbit anti-Sec10 antibodies or 2.5 μg mAb against Sec8 were added for 30 min at 4°C. Then, protein G–Sepharose beads (Amersham Biosciences) were added, incubated for 5 h at 4°C, and washed three times in lysis buffer and once in 50 mM Tris, pH 7.5. Proteins were separated on 8% polyacrylamide gels and transferred to PVDF membranes. Detection of bound antibodies was performed with the ECL procedure (Amersham Biosciences).

Online supplemental material

Fig. S1 shows the characterization of anti-Sec10 pAbs. Fig. S2 shows the characterization of MDCK Tet-Off™ cells (clone 15) stably transformed with HA-tagged ARF6-Q67L. The online supplemental material is available at http://www.jcb.org/cgi/content/full/jcb.200305029/DC1.

We are indebted to M. Perderiset and L. Cabanié for help with ARF6 purification, J. Ménetrey and M. Franco for help with ARF6 nucleotide loading experiments, and M. Grasset (Centre Interuniversitaire de Microscopie Electronique, Paris, France) for assistance with scanning EM. We also thank Drs. J.-B. Sibarita and V. Fraisier (Institut Curie) for advice with confocal microscopy and cell area measurement. Drs. V.W. Hsu, S-C. Hsu, P. De Camilli, and G. Banting are acknowledged for gifts of reagents. We are grateful to Drs. F. Niedergang, J. Plastino, and T. Galli for critical reading of the manuscript.

This work was supported by institutional funding from Centre National de la Recherche Scientifique (CNRS) and Institut National de la Santé et de la Recherche Médicale (INSERM), and by grants from Institut Curie, the Fondation BNP Paribas, and the Ligue Nationale contre le Cancer (équipe labellisée) to P. Chavrier. T. Dubois was the recipient of a post-doctoral fellowship from Association pour la Recherche sur le Cancer.

Submitted: 7 May 2003
Accepted: 16 October 2003

References

Al-Awar, O., H. Radhakrishna, N.N. Powell, and J.G. Donaldson. 2000. Separation of membrane trafficking and actin remodeling functions of ARF6 with an effector domain mutant. *Mol. Cell. Biol.* 20:5998–6007.

Bajno, L., X.R. Peng, A.D. Schreiber, H.P. Moore, W.S. Trimble, and S. Grinstein. 2000. Focal exocytosis of VAMP3-containing vesicles at sites of phagosome formation. *J. Cell Biol.* 149:697–706.

Bretscher, M.S. 1996. Getting membrane flow and the cytoskeleton to cooperate in moving cells. *Cell.* 87:601–606.

Brymora, A., V.A. Valova, M.R. Larsen, B.D. Roufogalis, and P.J. Robinson. 2001. The brain exocyst complex interacts with RalA in a GTP-dependent manner: identification of a novel mammalian Sec3 gene and a second Sec15 gene. *J. Biol. Chem.* 276:29792–29797.

Chavrier, P., and B. Goud. 1999. The role of ARF and rab GTPases in membrane transport. *Curr. Opin. Cell Biol.* 11:466–475.

Chavrier, P., and M. Franco. 2001. Expression, purification, and biochemical properties of EFA6, a Sec7 domain-containing guanine exchange factor for ADP-ribosylation factor 6 (ARF6). *Methods Enzymol.* 329:272–279.

D'Souza-Schorey, C., G. Li, M.I. Colombo, and P.D. Stahl. 1995. A regulatory role for ARF6 in receptor-mediated endocytosis. *Science.* 267:1175–1178.

D'Souza-Schorey, C., E. van Donselaar, V.W. Hsu, C. Yang, P.D. Stahl, and P.J. Peters. 1998. ARF6 targets recycling vesicles to the plasma membrane: insights from an ultrastructural investigation. *J. Cell Biol.* 140:603–616.

Daro, E., P. Van der Sluijs, T. Galli, and I. Mellman. 1996. Rab4 and cellubrevin define different early endosome populations on the pathway of transferrin receptor recycling. *Proc. Natl. Acad. Sci. USA.* 93:9559–9564.

Elbashir, S.M., J. Harborth, W. Lendeckel, A. Yalcin, K. Weber, and T. Tuschl. 2001. Duplexes of 21-nucleotide RNAs mediate RNA interference in cultured mammalian cells. *Nature.* 411:494–498.

Finger, F.P., and P. Novick. 1998. Spatial regulation of exocytosis: lessons from yeast. *J. Cell Biol.* 142:609–612.

Finger, F.P., T.E. Hughes, and P. Novick. 1998. Sec3p is a spatial landmark for polarized secretion in budding yeast. *Cell.* 92:559–571.

Folsch, H., M. Pypaert, S. Maday, L. Pelletier, and I. Mellman. 2003. The AP-1A and AP-1B clathrin adaptor complexes define biochemically and functionally distinct membrane domains. *J. Cell Biol.* 163:351–362.

Franco, M., P.J. Peters, J. Boretto, E. van Donselaar, A. Neri, C. D'Souza-Schorey, and P. Chavrier. 1999. EFA6, a sec7 domain-containing exchange factor for ARF6, coordinates membrane recycling and actin cytoskeleton organization. *EMBO J.* 18:1480–1491.

Frank, S., S. Upender, S.H. Hansen, and J.E. Casanova. 1998. ARNO is a guanine nucleotide exchange factor for ADP-ribosylation factor 6. *J. Biol. Chem.* 273:23–27.

Grindstaff, K.K., C. Yeaman, N. Anandasabapathy, S.C. Hsu, E. Rodriguez-Boulan, R.H. Scheller, and W.J. Nelson. 1998. Sec6/8 complex is recruited to cell-cell contacts and specifies transport vesicle delivery to the basal-lateral membrane in epithelial cells. *Cell.* 93:731–740.

Grote, E., C.M. Carr, and P.J. Novick. 2000. Ordering the final events in yeast exocytosis. *J. Cell Biol.* 151:439–452.

Guillemot, J.C., P. Montcourrier, E. Vivier, J. Davoust, and P. Chavrier. 1997. Selective control of membrane ruffling and actin plaque assembly by the Rho GTPases Rac1 and CDC42 in FcεRI-activated rat basophilic leukemia (RBL-2H3) cells. *J. Cell Sci.* 110:2215–2225.

Guo, W., D. Roth, E. Gatti, P. De Camilli, and P. Novick. 1997. Identification and characterization of homologues of the Exocyst component Sec10p. *FEBS Lett.* 404:135–139.

Guo, W., A. Grant, and P. Novick. 1999a. Exo84p is an exocyst protein essential for secretion. *J. Biol. Chem.* 274:23558–23564.

Guo, W., D. Roth, C. Walch-Solimena, and P. Novick. 1999b. The exocyst is an effector for Sec4p, targeting secretory vesicles to sites of exocytosis. *EMBO J.* 18:1071–1080.

Guo, W., F. Tamanoi, and P. Novick. 2001. Spatial regulation of the exocyst complex by Rho1 GTPase. *Nat. Cell Biol.* 3:353–360.

Hazuka, C.D., D.L. Foletti, S.C. Hsu, Y. Kee, F.W. Hopf, and R.H. Scheller. 1999. The sec6/8 complex is located at neurite outgrowth and axonal synapse-assembly domains. *J. Neurosci.* 19:1324–1334.

Hopkins, C.R., A. Gibson, M. Shipman, D.K. Strickland, and I.S. Trowbridge. 1994. In migrating fibroblasts, recycling receptors are concentrated in narrow tubules in the pericentriolar area, and then routed to the plasma membrane of the leading lamella. *J. Cell Biol.* 125:1265–1274.

Inoue, M., L. Chang, J. Hwang, S.H. Chiang, and A.R. Saltiel. 2003. The exocyst complex is required for targeting of Glut4 to the plasma membrane by insulin. *Nature.* 422:629–633.

Kee, Y., J.S. Yoo, C.D. Hazuka, K.E. Peterson, S.C. Hsu, and R.H. Scheller. 1997. Subunit structure of the mammalian exocyst complex. *Proc. Natl. Acad. Sci. USA.* 94:14438–14443.

Laukaitis, C.M., D.J. Webb, K. Donais, and A.F. Horwitz. 2001. Differential dynamics of alpha 5 integrin, paxillin, and alpha-actinin during formation and disassembly of adhesions in migrating cells. *J. Cell Biol.* 153:1427–1440.

Lecuit, T., and F. Pilot. 2003. Developmental control of cell morphogenesis: a focus on membrane growth. *Nat. Cell Biol.* 5:103–108.

Lin, S.X., G.G. Gundersen, and F.R. Maxfield. 2002. Export from pericentriolar endocytic recycling compartment to cell surface depends on stable, detyrosinated (glu) microtubules and kinesin. *Mol. Biol. Cell.* 13:96–109.

Lipschutz, J.H., and K.E. Mostov. 2002. Exocytosis: the many masters of the exocyst. *Curr. Biol.* 12:R212–R214.

Lipschutz, J.H., W. Guo, L.E. O'Brien, Y.H. Nguyen, P. Novick, and K.E. Mostov. 2000. Exocyst is involved in cystogenesis and tubulogenesis and acts by modulating synthesis and delivery of basolateral plasma membrane and secretory proteins. *Mol. Biol. Cell.* 11:4259–4275.

Moskalenko, S., D.O. Henry, C. Rosse, G. Mirey, J.H. Camonis, and M.A. White. 2002. The exocyst is a Ral effector complex. *Nat. Cell Biol.* 4:66–72.

Moskalenko, S., C. Tong, C. Rosse, J. Camonis, and M.A. White. 2003. Ral GTPases regulate exocyst assembly through dual subunit interactions. *J. Biol. Chem.* In press.

Naslavsky, N., R. Weigert, and J.G. Donaldson. 2003. Convergence of non-clathrin- and clathrin-derived endosomes involves Arf6 inactivation and changes in phosphoinositides. *Mol. Biol. Cell.* 14:417–431.

Niedergang, F., E. Colucci-Guyon, T. Dubois, G. Raposo, and P. Chavrier. 2003.

ADP ribosylation factor 6 is activated and controls membrane delivery during phagocytosis in macrophages. *J. Cell Biol.* 161:1143–1150.

Novick, P., and W. Guo. 2002. Ras family therapy: Rab, Rho and Ral talk to the exocyst. *Trends Cell Biol.* 12:247–249.

Palacios, F., L. Price, J. Schweitzer, J. Collard, and C. D'Souza-Schorey. 2001. An essential role for ARF6-regulated membrane traffic in adherens junction turnover and epithelial cell migration. *EMBO J.* 20:4973–4986.

Pierini, L.M., M.A. Lawson, R.J. Eddy, B. Hendey, and F.R. Maxfield. 2000. Oriented endocytic recycling of α5β1 in motile neutrophils. *Blood.* 95: 2471–2480.

Radhakrishna, H., and J.G. Donaldson. 1997. ADP-ribosylation factor 6 regulates a novel plasma membrane recycling pathway. *J. Cell Biol.* 139:49–61.

Radhakrishna, H., O. Al-Awar, Z. Khachikian, and J.G. Donaldson. 1999. ARF6 requirement for Rac ruffling suggests a role for membrane trafficking in cortical actin rearrangements. *J. Cell Sci.* 112:855–866.

Raposo, G., M.J. Kleijmeer, G. Posthuma, J.W. Slot, and H.J. Geuze. 1997. Immunogold labeling of ultrathin cryosections: application in immunology. *In* Weir's Handbook of Experimental Immunology. L.A. Herzenberg, D.M. Weir, and C. Blackwell, editors. Blackwell Science Inc., Malden, MA. 208.1–208.11.

Roberts, M., S. Barry, A. Woods, P. van der Sluijs, and J. Norman. 2001. PDGF-regulated rab4-dependent recycling of αvβ3 integrin from early endosomes is necessary for cell adhesion and spreading. *Curr. Biol.* 11:1392–1402.

Roth, D., W. Guo, and P. Novick. 1998. Dominant negative alleles of SEC10 reveal distinct domains involved in secretion and morphogenesis in yeast. *Mol. Biol. Cell.* 9:1725–1739.

Santy, L.C., and J.E. Casanova. 2001. Activation of ARF6 by ARNO stimulates epithelial cell migration through downstream activation of both Rac1 and phospholipase D. *J. Cell Biol.* 154:599–610.

Sheff, D.R., E.A. Daro, M. Hull, and I. Mellman. 1999. The receptor recycling pathway contains two distinct populations of early endosomes with different sorting functions. *J. Cell Biol.* 145:123–139.

Song, J., Z. Khachikian, H. Radhakrishna, and J.G. Donaldson. 1998. Localization of endogenous ARF6 to sites of cortical actin rearrangement and involvement of ARF6 in cell spreading. *J. Cell Sci.* 111:2257–2267.

Stoorvogel, W., V. Oorschot, and H.J. Geuze. 1996. A novel class of clathrin-coated vesicles budding from endosomes. *J. Cell Biol.* 132:21–33.

TerBush, D.R., and P. Novick. 1995. Sec6, Sec8, and Sec15 are components of a multisubunit complex which localizes to small bud tips in *Saccharomyces cerevisiae*. *J. Cell Biol.* 130:299–312.

Vega, I.E., and S.C. Hsu. 2001. The exocyst complex associates with microtubules to mediate vesicle targeting and neurite outgrowth. *J. Neurosci.* 21:3839–3848.

Vitale, N., S. Chasserot-Golaz, Y. Bailly, N. Morinaga, M.A. Frohman, and M.F. Bader. 2002. Calcium-regulated exocytosis of dense-core vesicles requires the activation of ADP-ribosylation factor (ARF)6 by ARF nucleotide binding site opener at the plasma membrane. *J. Cell Biol.* 159:79–89.

Vojtek, A.B., and S.M. Hollenberg. 1995. Ras-Raf interaction: two-hybrid analysis. *Methods Enzymol.* 255:331–342.

Yang, C.Z., and M. Mueckler. 1999. ADP-ribosylation factor 6 (ARF6) defines two insulin-regulated secretory pathways in adipocytes. *J. Biol. Chem.* 274: 25297–25300.

Yeaman, C., K.K. Grindstaff, J.R. Wright, and W.J. Nelson. 2001. Sec6/8 complexes on trans-Golgi network and plasma membrane regulate late stages of exocytosis in mammalian cells. *J. Cell Biol.* 155:593–604.

Zhang, Q., D. Cox, C.C. Tseng, J.G. Donaldson, and S. Greenberg. 1998. A requirement for ARF6 in fcγ receptor-mediated phagocytosis in macrophages. *J. Biol. Chem.* 273:19977–19981.

Zhang, X., E. Bi, P. Novick, L. Du, K.G. Kozminski, J.H. Lipschutz, and W. Guo. 2001. Cdc42 interacts with the exocyst and regulates polarized secretion. *J. Biol. Chem.* 276:46745–46750.